Proteomics Links the Redox State to Calcium Signaling During Bleaching of the Scleractinian Coral *Acropora microphthalma* on Exposure to High Solar Irradiance and Thermal Stress⑤

Andrew J. Weston‡§§, Walter C. Dunlap§‖, Victor H. Beltran§¶, Antonio Starcevic‡‡, Daslav Hranueli‡‡, Malcolm Ward‡, and Paul F. Long‖*

Shipboard experiments were each performed over a 2 day period to examine the proteomic response of the symbiotic coral *Acropora microphthalma* exposed to acute conditions of high temperature/low light or high light/low temperature stress. During these treatments, corals had noticeably bleached. The photosynthetic performance of residual algal endosymbionts was severely impaired but showed signs of recovery in both treatments by the end of the second day. Changes in the coral proteome were determined daily and, using recently available annotated genome sequences, the individual contributions of the coral host and algal endosymbionts could be extracted from these data. Quantitative changes in proteins relevant to redox state and calcium metabolism are presented. Notably, expression of common antioxidant proteins was not detected from the coral host but present in the algal endosymbiont proteome. Possible roles for elevated carbonic anhydrase in the coral host are considered: to restore intracellular pH diminished by loss of photosynthetic activity, to indirectly limit intracellular calcium influx linked with enhanced calmodulin expression to impede late-stage symbiont exocytosis, or to enhance inorganic carbon transport to improve the photosynthetic performance of algal symbionts that remain *in hospite*. Protein effectors of calcium-dependent exocytosis were present in both symbiotic partners. No caspase-family proteins associated with host cell apoptosis, with exception of the autophagy chaperone HSP70, were detected, suggesting that algal loss and photosynthetic dysfunction under these experimental conditions were not due to host-mediated phytosymbiont destruction. Instead, bleaching occurred by symbiont exocytosis and loss of light-harvesting pigments of algae that remain *in hospite*. These proteomic data are, therefore, consistent with our premise that coral endosymbionts can mediate their own retention or departure from the coral host, which may manifest as "symbiont shuffling" of *Symbiodinium* clades in response to environmental stress. *Molecular & Cellular Proteomics 14: 10.1074/mcp.M114.043125, 585–595, 2015.*

From the ‡King's College London Proteomics Facility, Institute of Psychiatry, London SE5 8AF, UK. §Centre for Marine Microbiology and Genetics, Australian Institute of Marine Science, PMB No. 3 Townsville MC, Townsville, Queensland,4810 Australia. ¶ARC Centre of Excellence for Coral Reef Studies, James Cook University, Townsville QLD 4811 Australia. ‡‡Section for Bioinformatics, Department of Biochemical Engineering, Faculty of Food Technology & Biotechnology, University of Zagreb, Pierottijeva 6, HR-10000 Zagreb, Croatia. ‖Institute of Pharmaceutical Science, Kings College, Strand, London WC2R 2LS, United Kingdom, **Department of Chemistry, King's College Strand, London WC2R 2LS, United Kingdom, Franklin-Wilkins Building, Stamford Street, London SE1 9NH, UK

The success of reef-building corals and that of other symbiotic cnidarians depends on metabolic cooperation between the animal host and endosymbiotic algae residing within its cells. Breakdown of this symbiosis in corals under conditions of environmental stress is manifested as bleaching (loss of endosymbionts or photosynthetic pigments), and eventual death of the colony occurs if the association is not re-established, thereby threatening the persistence of coral reef ecosystems. Even if the symbiosis is re-established, growth and reproduction may be impaired for long afterward (1). Because we are in the midst of alarming losses of coral reefs owing to mounting levels of environmental stress, a much fuller understanding is required to appreciate how coral symbiosis is regulated if we are to predict the impact of environmental change on the future resilience of tropical coral reef ecosystems (2).

In the mutualistic partnership of cnidarian-algal symbiosis, symbiotic dinoflagellates of the genus *Symbiodinium* (colloquially known as zooxanthellae and abbreviated to Zx) grow and proliferate within a specialized phagosome (the symbiosome) of cnidarian gastrodermal cells (3). In order to reside in this intracellular niche, the symbiosome and resident Zx are

co-adapted so that symbiotic algae resist phagocytotic digestion and the host allows the transport of essential nutrients and waste products across the symbiosome membrane to sustain the metabolism, growth, and reproduction of the algal endosymbionts, which in turn release photosynthetically fixed carbon to the host for nutrition.

There are five separate cellular mechanisms postulated for the loss of endosymbionts from cnidarian host tissues by stress-induced bleaching: *in situ* symbiont degradation and digestion, symbiont exocytosis, host cell detachment, host cell necrosis, and host cell apoptosis (4). While apoptotic cell death and autophagy are favored by some contemporary coral reef scientists as the proximal cause of coral bleaching (5–7), histological examination provides clear evidence that coral host cells *in situ* are not significantly degraded by apoptosis during environmentally relevant bleaching conditions (8), that zooxanthellae are released from the endoderm into the coelenteron cavity in partially bleached corals (9), and that endosymbionts freshly expelled during thermal bleaching may even appear healthy and are photosynthetically competent (10, 11).

Exocytosis has an absolute requirement for a sustained influx of Ca^{2+}, the intracellular concentration of which is regulated by the Ca^{2+} binding proteins calmodulin and synaptotagmin (12). Down-regulation of calmodulin gene expression has been shown under conditions of induced oxidative stress in the bleaching response of the coral *Montastraea faveolata*, although disruption in Ca^{2+} homeostasis was not demonstrated in that transcriptomics experiment (13). Additionally, in a differential gene-expression experiment designed to examine the molecular response of the coral *Acropora microphthalma* to enhanced levels of solar irradiance, we have observed enhanced transcription of a Ca^{2+}-binding, synaptotagmin-like regulator of SNARE protein assembly in solar-exposed colonies during the early stages of coral bleaching (14). These two results are consistent with the regulatory roles of calmodulin and synaptotagmin in Ca^{2+}/SNARE-dependent exocytosis (15).

We have also reported evidence for the existence of proteins required for exocytosis in a symbiont-enriched fraction of the coral *Stylophora pistillata* (16). These proteins included antagonistic vesicular and target SNARE proteins that, by comparative proteomic analysis using the recently released ZoophyteBase annotation of the *Acropora digitifera* proteome (17), appear to be encoded either by the host (target SNAREs) or symbiont (vesicular SNAREs). We posit that SNARE assembly utilizes vesicular SNARE proteins of the endosymbiont enabling stress-sensitive endosymbionts to mediate their own exit from the host, which departs from customary thinking that the host unilaterally expels its symbionts.

It is well accepted that oxidative stress is the proximal cause for the collapse of symbiosis in coral bleaching (18). Yet, evidence for a direct link between oxidative stress and the cytosolic influx of Ca^{2+} required for exocytosis is at best equivocal. Sawyer and Muscatine (19) did not find any change in intracellular Ca^{2+} or host cell detachment in the tropical sea anemone *Aiptasia pulchella* during thermal-induced coral bleaching. However, Fang *et al.* (10) did observe cytosolic influx of Ca^{2+} at high temperatures consistent with bleaching, although these experiments were performed on symbiont-free cells of the coral *Acropora grandis*. Likewise, Huang *et al.* (20) observed cytosolic influx of Ca^{2+} at the onset of bleaching while studying the intact holobiome of *A. grandis* and ventured that the loss of symbionts from the coral tissue as a result of heat shock could be attributed to an exocytosis mechanism. In the present experiment, we sought proteomic evidence to link elements of the symbiome redox state with molecular processes of coral bleaching in general and the involvement of Ca^{2+} regulation in particular.

EXPERIMENTAL PROCEDURES

Coral Collection and Experimental Design—A large colony of *Acropora microphthalma* (21) was selected from a depth of 12.7 m (mid tide) at Davies Reef in the central region of the Great Barrier Reef, Australia (147° 37.778′ E : 18° 49.270′ S). Three mid-sized healthy fragments from this colony were brought to the surface and arranged on plastic-coated metal dish racks. These racks were distributed within a sun-exposed 600-liter tank at a depth of 40 cm in constantly pumped and thermally adjusted water taken from the seawater supply of the Australian Institute of Marine Science ship RV *Cape Ferguson*. This sampling was repeated three times so that the photobiological response of the colony fragments could be determined on exposure to three different combinations of stress conditions: high light and low temperature using ambient seawater at 26 °C (seawater is usually well mixed in the upper 20 m of the Great Barrier Reef during wintertime turbulence and so would be similar to temperature at the collection depth); high light and high temperature by heating the tank seawater (31 °C max.); and low light with high temperature, again by heating the tank seawater (31 °C max.). In full sunlight, corals received up to 2,000 μmol photons m^{-2} s^{-1} of photosynthetic active radiation (PAR) at noon, with an average PAR exposure measured hourly during daylight hours of 466 μmol photons m^{-2} s^{-1} during the day for those corals exposed to high light conditions. For corals that were exposed to low light, a 70% shade cloth filter placed above the tank gave an average exposure of 157 μE during the day, which approximates the irradiance at the coral's natural (10–15 m) habitat. The seawater temperature was adjusted to 31 °C during the day and lowered to 28 °C at night (to approach natural conditions) for high temperature treatments using an inline temperature-controlled, heater/pump device providing 120 l min^{-1} of water displacement.

ITS1 single-stranded conformational polymorphism (ITS1-SSCP) analysis (22, 23) was used to determine the dinoflagellate clade type (ITS1 standard: GenBank EU024793). To follow the stress-induced photosynthetic performance of the algal symbionts *in hospite* we used a Pulse Amplified Modulated Fluorometer (Diving PAM, Heinz Walz GmbH, Effeltrich, Germany) for measuring photophysiological parameters. Light-adapted photosystem II quantum yield and maximum effective quantum yield ($\Delta F/F_m$') was recorded three times a day (morning at 8am; noon at 12 pm; afternoon at 5 pm) at eight uniformly pigmented locations on branches of each of the coral fragments. In these three 2-day experiments, tissues from the holobiont to be used for proteomic analyses were removed at time points t = 0 (26 °C), t = 1 after 12 h of acclimatization with high or low light at either 26 °C or 31° on day 1 and t = 2 after 12 h of acclimatization at either 26 °C or

31° on day 2 to give a total of nine samples for this experiment. Coral tissue was removed by blasting with a 40 ml solution of 0.02% SDS (w/v) in Ca^{2+}-free sterile seawater under a jet of compressed air. The tissue slurry was homogenized and filtered through a 180 μm screen to remove skeletal fragments. To 9.8 ml aliquots, 100 μl 0.5 M EDTA and 100 μl Halt Protease and Phosphatase Inhibitor Mixture (Thermo Scientific, Wilmington, DE, USA) were added, and the aliquots were frozen in liquid nitrogen for transport back to the laboratory for further processing. Handling and processing time for each sample did not exceed 10 min.

Protein Extraction from Corals—Approximately 100 μl of glass beads (Sigma-Aldrich, Dorest, UK) were added to each 10 ml of tissue sample. Each sample was vortexed for 1 min and then placed on ice for 1 min. The procedure was repeated ten times. The suspension was then transferred to a conical tube and centrifuged at 16,000 $\times$ g for 10 min at 4 °C. The supernatant, which contained soluble proteins, was decanted and lyophilized. Insoluble proteins from the pellet were solubilized using 8 M urea and the suspension was then lyophilized. The lyophilized materials comprising both the soluble and insoluble fractions were both reconstituted in 200 μl 50 mM TEAB (triethylammonium bicarbonate). The proteins were precipitated from these solutions using two volumes of acetone at −80 °C for 2 h. Following centrifugation at 16,000 $\times$ g for 5 min, the acetone was removed and the pellets were allowed to dry. The pellets were dissolved again in 50 mM TEAB, and a nanodrop (Thermo Scientific, Wilmington, DE, USA) assay was performed to determine protein concentration.

TMT Labeling—A tandem mass tag (TMT) six-plex intact protein labeling kit (ThermoFisher Scientific, Rockford, IL, USA) was used to quantify fold-changes in protein concentrations between reference and experimental treatments. Each tag was reconstituted in 24 μl of acetonitrile and equilibrated at room temperature before adding TMT reagents to each sample. Three reference samples were prepared by pooling 12 μg of protein from the soluble fraction of all nine treatment samples. Three reference samples were also prepared in the same way using the insoluble fractions from all nine treatment samples. The three pooled reference samples and the nine individual samples were labeled by the addition of each tag to give the equivalent of 36 μg of protein per sample. The samples were then lyophilized and reconstituted in 50 μl of 50 mM TEAB containing 0.04% SDS for re-solubilization. The samples were then reduced by adding 5 μl of 9 mM tris(2-carboxyethyl)phosphine hydrochloride in 50 mM TEAB at 55 °C for 1 h, then alkylated with 5 μl of 16 mM iodoacetamide in 50 mM TEAB in the dark at room temperature for 30 min. A volume of 8 μl of 5% hydroxylamine (w/w) was added according to TMT procedures to terminate the reaction. The three pooled reference samples and the nine individual samples were pooled and mixed into two separate tubes as follows: Tube 1 contained a reference plus samples representing time points t = 0, t = 1, and t = 2 from the high light and low temperature treatment as well as time points t = 1 and t = 2 from the high light and high temperature treatment. Tube 2 contained two reference samples plus samples representing time points t = 0, t = 1, and t = 2 from the low light with high temperature treatment as well as time points t = 0 from the high light and high temperature treatment. The procedure was repeated for soluble and insoluble fractions giving a total of four tubes, each containing six-plex reactions. After mixing the samples, the solutions were lyophilized. Excess TMT reagent was removed from these samples during protein SDS-PAGE separation.

1D Gel Fractionation and In-Gel Digestion—The six-plex TMT-labeled mixtures were reconstituted in 40 μl TEAB and 40 μl Laemmli buffer (24) and heated at 70 °C for 5 min before loading across four lanes of a 4–12% NuPAGE Novex Bis-Tris gel (Invitrogen, Paisley, UK) with MES buffer alongside Novex® SeeBlue® Plus2 prestained standards (Invitrogen). Electrophoresis was carried out for 120 min at 150 V. The gel was fixed, stained with Coomassie Blue, destained, and visualized with ImageQuant (GE Healthcare, Buckinghamshire, UK). Bands were then selected for excision and in-gel digestion. The gel lanes were sectioned into ten portions giving a total of 40 samples for quantitative processing (ten gel fractions $\times$ two cellular fractions $\times$ two six-plex reactions comprising all three conditions). In-gel reduction, alkylation, and proteolytic digestion with trypsin were performed prior to subsequent analysis by mass spectrometry as follows (25). Briefly, cysteine residues were reduced with 10 mM dithiothreitol and alkylated with 55 mM iodoacetamide in 100 mM ammonium bicarbonate to form stable carbamidomethyl derivatives. Trypsin digestion of each section was carried out overnight at 37 °C in 50 mM ammonium carbonate buffer, and the supernatant was retained. Peptides were extracted from the excised gel portions by two treatments with 50 mM ammonium bicarbonate and acetonitrile. Each treatment involved shaking gel sections for 15 min before collecting the peptide-containing extract. The extract was pooled with the initial digestion supernatant and then lyophilized.

LC-MS/MS—Samples were reconstituted in 60 μl 0.1% formic acid and 3% acetonitrile, centrifuged and 5 μl of the particle-free supernatant was injected into a Thermo Scientific LTQ Orbitrap Velos mass spectrometer coupled to an EASY-nLC II (Proxeon) nano-LC instrument. A top 20 data-dependent mass spectrometry method with Higher-energy collisional dissociation (HCD) fragmentation was used together with a 1 h LC gradient. Samples were trapped on a 0.1 $\times$ 20 mm self-packed column filled with ReproSil C18, 5 μm (Dr. Maisch, Ammerbuch-Entringen, Germany). After loading and washing of the samples the separation was run on a 0.075 $\times$ 150 mm self-packed column filled with ReproSil C18, 3 μm (Dr. Maisch) for 45 min using a gradient ranging from 5% to 30% of 99.9% acetonitrile: 0.1% formic acid in 99.9% H_2O : 0.1% formic acid at a flow rate of 300 nl min^{-1}. For the CID method, MS spectra ranging from 400 to 1800 Da (m/z) were acquired in the Orbitrap at a resolution of 30,000 and the 20 most intense ions were subjected to MS/MS by CID fragmentation in the ion trap using a threshold of 5,000 counts. Isolation width of precursor selection was set at 2 units. Normalized collision energy for peptides was set at 35 units. Automatic gain control settings for FTMS survey scans were $10e^6$ counts and for FT MS/MS scans the gain control settings were $1e^4$ counts. Maximum injection time was 500 ms for survey scans and 100 ms for MS/MS scans. Unassigned and +1 charged ions were excluded for MS/MS and a dynamic exclusion list with a duration of 30 s was applied.

Data Analysis—'Rawfiles' from mass spectrometry analysis were processed for database spectral matching using Proteome Discoverer (version 1.4; Thermo Scientific). Mascot software (version 2.2.03; Matrix Science, London, UK) was used as the search algorithm with the following variable modifications: methionine oxidation, phosphorylation on S/T/Y, deamidation on N/D plus intact TMT-6plex quantitation (TMT-lysine). Carbamidomethyl cysteine was selected as a fixed modification. A digestion enzyme of trypsin was set allowing up to two missed cleavages. The data were searched with a parent ion tolerance of 5 ppm and a fragment ion tolerance of 0.02 Da. Raw files from a single gel lane were merged by Proteome Discoverer giving 4 search files corresponding to the two TMT-labeled mixes for both supernatant and pellet fractions. The data were annotated by searching against the *Symbiodinium minutum* Clade B1 predicted proteome sequence (26) to represent the Zx fraction of the symbiome, and a custom database of genomic *A. digitifera* annotation (17) was used to identify coral host proteins. Remaining peptides that did not have homology to either Zx or host were annotated as protein with homology to microbial or eukaryotic proteins by searching the Uniprot reference database (http://www.uniprot.org/help/uniprotkb). For quantitative analysis, the Mascot peptide summary report from the merged data was exported as a comma-separated values (.csv) file.

An in-house PERL script was then used to merge the .csv file and tab-separated values (.tsv) file from the search that contained the TMT intensities. All Mascot peptide identifications of any score and probability-based expected value were accepted meeting the following criteria: all peptides rank 1, flagged as bold or K-containing peptides with one or more detected tags. Grouping of peptides matched to multiple database entries was not reported. Instead, the assignment declared first in the Mascot peptide summary report was used. Also, using rank 1, bold red peptides ensured that peptides reported were based on the highest-scoring assignments. False discovery rates were not used because peptides assigned to multiple database entries were excluded from further analysis.

Exported quantitative data from the two tubes corresponding to each fraction were then merged and data grouped according to protein description. This gave files containing quantitative information for nine samples and three references for the soluble fraction and nine samples and three references for the insoluble fraction. Ratios of time points $t = 1$ and $t = 2$ to time point $t = 0$ were taken for each MS/MS event for high light with low temperature and low light with high temperature treatments since both treatments had samples representing all three time points mixed either into tube 1 or tube 2, respectively. The samples from the high light with high temperature treatment were separated across the two tubes with time points $t = 1$ and $t = 2$ in tube 1 and time point $t = 0$ in tube 2, thus ratios for this treatment could not be calculated directly. The TMT values for these samples were normalized using the pooled reference sample TMT values in the respective tubes. Time points $t = 1$ and $t = 2$ (high light with high temperature treatment) were normalized according to the reference sample in tube 1. Time point $t = 0$ (high light and high temperature treatment) was normalized according to the average of the two references in tube 2. A separate PERL script was then used to take averages of the same TMT intensity ratios for each MS/MS event assigned to the same protein in the high light with low temperature and low light with high temperature treatments. A PERL script was also used to take averages of the normalized tag intensities for each MS/MS event assigned to the same protein in the high light with high temperature treatment. The ratios of the averaged TMT intensities for the high light with high temperature treatment were then calculated from the resulting Excel file. This enabled a calculation of fold changes per annotated protein between the three time points for each of the three conditions.

<div align="center">RESULTS</div>

Quantitative Proteomics Overview—The MS/MS spectra for protein identifications are shown in SI Dataset 1. The average fold-change of the TMT intensities for each treatment relative to the unstressed $t = 0$ proteome were calculated for all peptides assigned to the same protein across two, or better, three replicates (SI Dataset 2: coral host; SI Dataset 3: all symbionts). Unfortunately, although peptides from the high light/high temperature treatment could be annotated (SI Dataset 4: complete proteome), the reliability of data for these expressed peptides could not meet our stringent criteria for quantification, and so data from this harsh treatment were omitted from further empirical consideration. Peptides could be quantified from the other two stress treatments, and these peptides were then grouped according to probable organism-of-origin and likely biochemical function by comparison with three relevant peptide databases. The average fold-change of peptides associated with redox state and Ca^{2+} metabolism, including signaling of exocytosis, are shown in Table 1, for

peptides of likely coral host origin, and in Table 2, for peptides of likely algal symbiont origin. All other peptides where fold-changes could be calculated are given in the supplemental data (SI Dataset 5: coral host peptides, SI Dataset 6: algal symbiont peptides, SI Dataset 7: prokaryote symbionts, SI Dataset 8: eukaryote symbionts). Values <1 or >1 indicated either a reduction or increase in tag intensity as compared with the unstressed $t = 0$ proteome, a value equal to 1 indicates no change in protein abundance, a value of 0 indicates the presence of a peptide in the unstressed $t = 0$ proteome but absence of the peptide in the treatment proteome and N/D indicates presence of a peptide in the treated proteome but absent in the unstressed $t = 0$ proteome. Overall, the trends in peptide fold-changes were the same for both the coral host and algal symbiont peptides. In the high temperature/low light treatment, the peptide fold-changes generally increased across the 2-day experiment compared with the unstressed $t = 0$ proteome. In contrast, the peptide-fold changes were massive in day 1 as compared with the unstressed $t = 0$ proteome in the high light/low temperature treatment, but these changes collapsed by day 2 for all but a few detectable peptides. This pattern in peptide fold-changes was consistent with photosystem II quantum yield measurements, indicating loss of photosynthetic function, and recovery (*Yr*) occurred more rapidly in the high temperature/low light treatment than did the high light/low temperature treatment.

Coral Host Proteins (Table 1)—The absence of common antioxidant proteins detected in the coral host quantitative dataset during high temperature/low light and high light/low temperature treatments was surprising. The enzymes choloylglycine hydrolase (KEGG ontology K01442) and carbonic anhydrase (KEGG ontology K01672) were both present in the unstressed $t = 0$ proteome for the high temperature/low light treatment, and both had huge 157-fold increases by day 1 but could not be detected by day 2. These enzymes were also present in the high light/low temperature treatment across both days, but quantification was not possible because these enzymes were not detected for the unstressed $t = 0$ proteome for this treatment dataset.

Quantitative changes in multiple host proteins that regulate vesicle exocytosis could be detected during the experiment. Membrane fusion is mediated by complementary SNARE proteins that are either vesicle-associated membrane proteins (vSNAREs) or corresponding proteins inserted into the target plasma membrane (tSNAREs). Only one vSNARE was detected (KEGG ontology K12314) for the high light/low temperature experiment, but the magnitude of its induction could not be quantified since it was not detected for the $t = 0$ unstressed proteome. This protein shows only a modest 2.3 fold increase on day 1 of the high temperature/low light experiment, before becoming undetectable on day 2. There were four different tSNARE proteins identified under both experimental conditions (KEGG ontologies K09290, K05865; two

TABLE I

Quantified changes of coral host proteins with putative antioxidant, calcification, or exocytosis functions in stress-treated Acropora microphthalm

Gene sequence	KEGG orthology	Encoded protein description	High light low temperature		Low light high temperature	
			Day 1	Day 2	Day 1	Day 2
(a) Antioxidant proteins						
v1.02821	K01442	*Choloylglycine hydrolase*	n/d	n/d	157.0	0.0
(b) Calcification proteins						
v1.16354	K01672	*Carbonic anhydrase*	n/d	n/d	157.0	0.0
(b) Exocytosis						
v1.13367	K12314	Actin alpha cardiac muscle ACTC1 protein (vSNARE)	n/d	n/d	2.3	0.0
v1.08398	K09290	Tropomyosin 3 cytoskeletal actin-binding protein (tSNARE)	0.5	1.7	52.7	0.1
v1.12307	K09290	Tropomyosin 3 cytoskeletal actin-binding protein (tSNARE)	12.9	40.2	93.6	0.0
v1.22045	K05865	Troponin C Ca^{2+}-receptor of tropomyosin (tSNARE)	1.4	2.4	n/d	n/d
v1.23189	K05865	Troponin C Ca^{2+}-receptor of tropomyosin (tSNARE)	n/d	n/d	91.9	0.0
v1.03896	K05316	Voltage-dependent calcium channel alpha-2/delta invertebrate-type protein	0.2	0.0	n/d	n/d
v1.13117	K04988	Polycystin 1L2 membrane G-protein-binding receptor of calcium homeostasis	0.6	1.8	n/d	n/d
v1.15901	K13448	Calcium-binding protein CML calcium CAM-like sensor signaling protein	1.0	3.4	96.8	0.0
v1.01102	K02183	Calmodulin calcium-binding messenger multifunctional signaling protein	77.9	106.2	n/d	n/d
v1.15351	K08886	Activated CDC42 kinase 1 non-receptor serine/threonine signaling kinase	n/d	n/d	156.9	0.0
v1.24588	K08287	Dual-specificity kinase protein tyrosine and serine/threonine activity	n/d	n/d	156.9	0.0
v1.05162	K13412	Calcium-dependent protein kinase mediator of Ca^{2+}/calmodulin signaling	1.4	5.5	68.3	0.0
v1.14153	K12478	Early endosome antigen 1 multivalent affector of Rab5A GTPase trafficking	n/d	n/d	39.8	0.0

A value of 0 indicates no tag intensity could be detected compared to the control, while n/d is no tag detected in the t = 0 unstressed proteome and so fold-change could not be calculated.

family-member proteins for each), all showing a similar pattern in fold-changes distinct to both treatments. Each increased from day 1 to day 2 during the high light/low temperature experiment, while a huge fold decrease occurred from day 1 to day 2 during the high temperature/low light experiment. Docking of the vesicle to the target membrane is Ca_2^+-dependent and two ion-channel proteins involved in Ca^{2+} regulation (KEGG ontologies K05316 and K04988) indeed were detected, although the fold-changes in these proteins are difficult to interpret. Premature vesicle docking is prevented by the binding of free Ca^{2+} to calmodulin, and only one family-member calmodulin protein was detected (KEGG ontology 13448), showing a modest fold increase from day 1 to day 2 during the high light/low temperature experiment, whereas a large decrease occurred from day 1 to day 2 during the high temperature/low light experiment.

Fast vesicle docking is conferred by the calmodulin antagonist synaptotagmins. None of these proteins were detected in the host proteome on initial annotation of the protein dataset, yet closer inspection revealed a calmodulin-like protein (KEGG ontology K02183) described in the Uniprot database as a calcium-binding calmodulin competitor (Uniprot accession number Q5U206). Expression of this protein would be consistent with observed large fold-changes in this protein for exocytosis to occur during coral bleaching. All of the effector proteins of vesicular trafficking require phosphorylation for

functional activity, and three kinase proteins consistent with this role were detected (KEGG ontologies K08886, K08287, and K13412), together with a Rab5A GTPase (KEGG ontology K12478) having an intrinsic regulatory role in the exocytosis process.

Algal Symbiont Proteins (Table 2)—A common mechanism for the detoxification of ROS oxidation products is the production of glutathione S-transferase (Uniprot accession number P28342) and thiol reductases, such as peroxiredoxins (Uniprot accession numbers Q5E947 and Q6DV14), both of which were detected in our dataset. Higher fold increases in these enzymes were expressed under both experimental treatments as compared to that of the unstressed t = 0 proteome, consistent with reactive oxygen species-induced initiation of coral bleaching. Xanthine dehydrogenase (Uniprot accession number Q54FB7) appeared also in our dataset. This enzyme catalyzes the formation of uric acid, which is a strong reductant and antioxidant. Xanthine dehydrogenase was detected likewise in the proteome of a symbiont-enriched fraction during experimental bleaching of the coral *S. pistillata* (16). Surprisingly, none of the common antioxidant enzymes such as superoxide dismutase, catalase, or ascorbate peroxidase were detected by our analytical method. Several heat shock proteins that are ATP-dependent molecular chaperones that function to maintain correct protein folding during cell stress were expressed with high fold increases during

TABLE II

Quantified changes of Symbiodinium proteins with putative antioxidant and cell stress or exocytosis functions in stress-treated Acropora microphthalma

Symbiodinium proteome					x-Fold-change in protein expression			
Uniprot accession number	Uniprot protein annotation	Accession number of SymB1 protein with greatest homology	BLASTp score	BLASTp e-value	High light low temperature		Low light high temperature	
					Day 1	Day 2	Day 1	Day 2
(a) Antioxidant and cell stress proteins								
P28342	Glutathione *S*-transferase 1 class zeta	v1.2.024109.t1	103	2e-22	n/d	n/d	24.2	2.1
Q5E947	Peroxiredoxin-1 of the thioredoxin system	v1.2.004521.t1 (+ 2 other sequences)	205	3e-53	3.6	6.6	n/d	n/d
Q6DV14	Peroxiredoxin-1 of the thioredoxin system	v1.2.004521.t1 (+ 2 other sequences)	205	3e-53	0.3	3.8	196.0	0.6
Q54FB7	Xanthine dehydrogenase/oxidase	v1.2.032465.t1 (+ 8 other sequences)	581	3e-165	1.0	1.4	n/d	n/d
(b) Exocytosis								
Q9XZP2	Calmodulin-2 of Ca^{2+}-signalling pathway	v1.2.025795.t1 (+ 27 other sequences)	284	4e-77	77.9	106.2	n/d	n/d
B0KIS5	Chaperone protein DnaK (HSP70)	v1.2.026933.t1 (+ 26 other sequences)	622	6e-178	0.6	3.4	n/d	n/d
Q7UM31	Chaperone protein DnaK (HSP70)	v1.2.026933.t1 (+ 27 other sequences)	630	1e-180	n/d	n/d	156.0	0.0
P06660	Heat shock-like 85 Da chaperone protein	v1.2.015892.t1 (+ 12 other sequences)	901	0.0	76.9	184.8	n/d	n/d
Q54DC8	Probable serine/threonine-protein kinase	v1.2.022894.t1 (+ 24 other sequences)	128	4e-29	1.2	0.7	n/d	n/d
O42632	Protein kinase C-like phosphorylase	v1.2.001451.t1 (+26 other sequences)	266	2e-70	1.4	7.4	n/d	n/d
Q12263	Serine/threonine-protein kinase GIN4	v1.2.020700.t1 (+ 26 other sequences)	258	3e-68	0.6	2.0	n/d	n/d
Q5F2E8	Serine/threonine-protein kinase TAO1 of MAPK	v1.2.009504.t1 (+ 27 other sequences)	145	2e-34	0.0	3.9	n/d	n/d

A value of 0 indicates no tag intensity could be detected compared to the control, while n/d is no tag detected in the t = 0 unstressed proteome and so fold-change could not be calculated.

treatment as compared to that of the unstressed t = 0 proteome. Unexpectedly, our heat- and light-stress treatments induced distinct HSP/chaperone proteins. DnaK, which is a member of the HSP70 family (Uniprot accession number Q7UM31), had a 156.0-fold increase on day 1 as compared to that of the unstressed t = 0 proteome in the high temperature/low light treatment, whereas the heat shock-like 85 Da chaperone protein (P06660) increased by 76.9 fold on day 1 and further increased to 184.8 fold by day 2 during the high light/low temperature treatment.

Active protein elements of exocytosis require ATP-dependent phosphorylation, which is catalyzed by protein kinases. Four kinases were detected (Uniprot accession numbers Q54DC8, O42632, Q12263, and Q5F2E8), which like the kinases assigned as proteins of host origin (Table 1), showed only small fold-changes consistent with low levels of constitutive expression. Calmodulin (calmodulin-2, Uniprot accession number Q9XZP2), which prevents Ca^{2+}-dependent assembly of the protein complex required for exocytosis by binding to free intracellular Ca^{2+}, showed massive 77.9 and 106.2 fold increases on day 1 and day 2, respectively, during the high light/low temperature treatment as compared to that of the unstressed t = 0 proteome. Calmodulin was also present in the high temperature/low light treatment, although ab-

solute changes could not be determined because the protein was not detected in the unstressed t = 0 proteome. Neither synaptotagmin agonists of calmodulin or, intriguingly, any other protein effectors of exocytosis were detected in the symbiont-derived proteomes of either treatment.

DISCUSSION

The intent of this study was to determine the proteomic response of the intact symbiome of the scleractinian coral *A. microphthalma* to solar irradiance and/or thermal stress. Particular interest was to quantify changes in the abundance of proteins associated with redox metabolism and Ca^{2+} sensing, including signaling of exocytosis during coral bleaching. For this purpose, experiments were performed where branches of *A. microphthalma* were exposed to seasonal sunlight equivalent to an average daytime surface PAR intensity of 466 μmol photons m^{-2} s^{-1} or reduced by shading to 157 μmol photons m^{-2} s^{-1}, which approximates the irradiance of the coral's natural 10–15m habitat. The sun exposed branches were maintained for the duration of each experiment in an shipboard tank that was supplied with a constant volume of fresh seawater kept at ambient (26 °C) or elevated (31 °C max.) temperatures. Hence, corals were exposed to high light/low temperature, high light/high temperature, or

high temperature/low light treatments. In these experiments, proteomics was used to investigate the molecular basis of symbiotic dysfunction in *A. microphthalma* during experimental conditions of elevated heat and light designed to promote a bleaching response. We have reported previously a comparison between the photosynthetic responses of four coral species common to the central Great Barrier Reef, including *A. microphthalma*, conducted concurrently during the course of these experiments (27). Briefly, the photosynthetic efficiency of the coral endosymbionts declined significantly in all treatments of this experiment, as evinced by reduced maximum effective quantum yields $(\Delta F/F_m')^1$ of photosystem II. This is consistent with the photophysical dysfunction of algal symbionts that precedes and progresses during coral bleaching. Yet, the rate of photosystem II yield recovery (*Yr*) showed this decline in photosynthetic efficiency was not consistent across all treatments for all corals examined. *Yr* determination revealed that *A. microphthalma* responds as a light tolerant but thermally sensitive species, with bleaching most severe under both high light and high temperature conditions; the degree of bleaching was greatest in the order: high light/high temperature > high temperature/low light > high light/low temperature.

The very recent availability of sequenced genomes for both the coral host (genus *Acropora*) and its algal endosymbiont (*Symbiodinium*) has enabled these data to be dissected to examine the likely response of each partner of the intact symbiome on exposure to specific conditions of abiotic stress. While proteomics has only recently emerged as a powerful tool to examine the molecular physiology of marine symbioses (16, 28–31), other biophysical techniques such as *in situ* pulse amplitude modulated fluorometry are well established to study photosynthetic function, symbiotic dysfunction and recovery in photoautotropic marine symbioses (32). Our pulse amplitude modulated fluorometry data (27) showed a clear stress-induced reduction in the photosynthetic performance of the algal symbionts of *A. microphthalma* residing *in hospite* that, together with visual examination of the coral tissues, confirmed that bleaching had occurred under all of the experimental conditions tested. However, the pulse amplitude modulated fluorometry data also showed that there was a measure of recovery in photosynthetic performance in both high light/low temperature and high temperature/low light treatments by t = 2 for each experiment, which would suggest that although algal symbionts could not be easily observed by gross visual inspection, there must remain a discrete population of viable algae in the host tissues. Bleaching was so rapid under

high light/high temperature conditions that quantitative proteomic data could not be obtained for the stressed symbiome. Future experiments may require shorter time intervals between sampling, particularly when examining high light/high temperature conditions. Additionally, the time period from collection of the coral specimens and acclimatization prior to treatment and sampling should be carefully monitored as this may affect the susceptibility of different corals to bleaching.

The same coral branches used for pulse amplitude modulated fluorometry determinations were also used for quantitative proteomics analyses. Under conditions of high temperature/low light or high light/low temperature treatment, peptides could be quantified and grouped according to probable organism-of-origin and likely biochemical function. Overall, the trends in peptide fold-changes were the same in proteomes attributed to the coral host, algal symbionts, and other coral associates of prokaryotic or eukaryotic origins (SI Datasets 5–8). For the high temperature/low light treatment, peptides generally showed a modest fold increase across the 2 day experiment compared to that of the unstressed control proteome. In contrast, peptide fold-changes for all probable organisms-of-origin were massive at t = 1 compared to that of the unstressed control proteome in the high light/low temperature treatment; however, these fold-changes collapsed by t = 2 with all but a few peptides being detectable. These patterns in peptide fold-changes were consistent with a greater decline of Fv/Fm' in the high temperature/low light treatment compared to that of the high light/low temperature treatment. These data suggest that since the same peptides could be quantified in each treatment and that the overall trend in peptide expression was the same in both treatments, then it is possible that the same mechanisms causing symbiotic dysfunction and recovery exist irrespective of the abiotic conditions causing the stress. In conjunction with the foregoing, similar fold-changes in diverse housekeeping proteins in host, Zx and other resident associates were also noted (SI Datasets 5–8) during these stress treatments, which would indicate an overall effect on cell physiological processes (such as protein synthesis) must be taken into account when considering coral resilience to conditions attributed to bleaching.

Algal endosymbionts produce oxygen in sunlight by photosynthesis in greater quantities than can be used for respiration by the coral host (33). Such hyperoxic coral tissues render both partners of photoautotrophic symbioses vulnerable to photooxidative stress caused by excess production of reactive oxygen species (34, 35). Antioxidant defenses include production of the enzymes superoxide dismutase and catalase, which are found in both partners (36) and peroxidases (ascorbate and glutathione) that are expressed by the algal symbiont (37). No common reactive oxygen species detoxification enzymes were detected in the quantitative coral host dataset (Table 1), which was surprising because both superoxide dismutase and catalase genes are encoded in the conspecific *A. digitifera* genome (17). Although the expression of
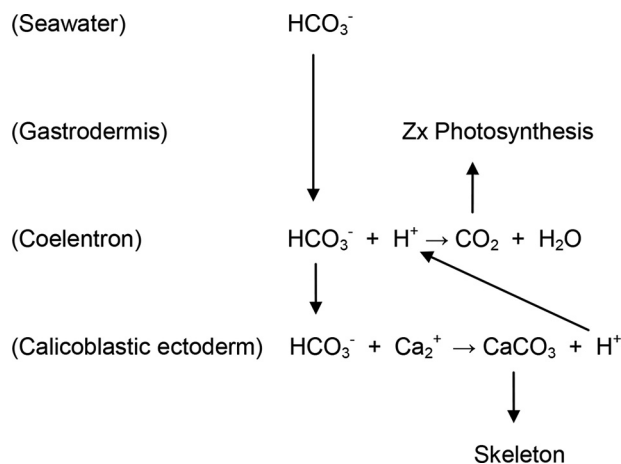
---

^{1} The abbreviations used are: $\Delta F/F_m'$: maximum effective quantum yield; ITS1-SSCP: ITS1 single-stranded conformational polymorphism analysis; PAR: photosynthetically active radiation (400–700 nm); SNARE: soluble NSF attachment receptor proteins; TEAB: triethylammonium bicarbonate; TMT: tandem mass tag (reagent); tSNARE: target SNARE protein; *Yr*: photosystem II yield recovery; vSNARE: vesicular SNARE protein; Zx: symbiotic dinoflagellates of the genus *Symbiodinium* (zooxanthellae).

choloylglycine hydrolase transcripts has been reported in *A. millipora* (38), a role for this enzyme in coral physiology has not yet been ascribed. In bacteria, this enzyme, which belongs to a class of enzymes known as the conjugated bile acid hydrolases, can hydrolyze glycocholic acid to glycine and cholic acid, for which the latter is known to have antioxidant activity (39). We suggest that choloylglycine hydrolase may provide an antioxidant function during coral recovery to replace more common antioxidant enzymes which may have been overwhelmed during extreme conditions of photooxidative stress. The only quantifiable proteins in the algal endosymbiont dataset (Table 2) that had antioxidant functions were thiol peroxidases consistent with previous experimental findings (16, 37). Present also in the quantitative algal symbiont dataset (Table 2) was xanthine dehydrogenase, which is a redox-interactive xanthine oxidoreductase enzyme that is converted to xanthine oxidase by reversible sulfhydryl oxidation or by irreversible proteolytic modification (40). Xanthine oxidase produces uric acid as an end product of purine catabolism. Uric acid is a strong reducing agent that may act as potent antioxidant, and expression of xanthine oxidase was likewise observed in an endosymbiont-enriched fraction of the coral *S. pistillata* during induced photooxidative stress (16).

Although the pH of the coral tissue was not measured in this experiment, the intracellular pH of the symbiotic scleractinian corals *Pocillopora damicornis* and *S. pistillata* has been measured at approximately pH 7.4 under ambient seasonal temperature, solar illumination, and natural seawater chemistry conditions (41, 42). In this study, both experimental conditions caused a significant decrease in photosynthetic efficiency (27). Such a decrease in photosynthetic activity causes acidosis at the calicoblastic ectoderm of corals as occurs during darkness (43, 44). In the coral *S. pistillata*, transcription of a gene encoding an extracellular carbonic anhydrase was up-regulated twofold during dark conditions at the calicoblastic ectoderm (45), which is the epithelium facing the skeleton that regulates calcification (46). In our experiment, carbonic anhydrase showed a 157-fold increase by t = 1 under conditions of high temperature and low light (Table 1). We suggest that this massive increase in carbonic anhydrase expression could be in response to bleached *A. microphthalma* tissues becoming acidic due to excessive CO_2 imbalance caused by host respiration as occurs naturally at night (33) or under conditions of depressed photosynthetic activity (41). Although contrary to what occurs in aposymbiotic anemones as compared with symbiotic conspecifics (47), increased carbonic anhydrase expression does occur normally at night in the scleractinian coral *S. pistillata* when algal photosynthesis is absent (48).

Carbonic anhydrase catalyzes the reversible hydration of CO_2 to $HCO_3^- + H^+$ and so is important in the supply of inorganic carbon to deposit the host $CaCO_3$ skeleton and by reverse hydration acts as a CO_2-concentrating mechanism to maintain symbiont photosynthesis (49). Simplified equations for these processes are:

(Seawater) HCO_3^-

(Gastrodermis)   Zx Photosynthesis

(Coelentron) $HCO_3^- + H^+ \rightarrow CO_2 + H_2O$

(Calicoblastic ectoderm) $HCO_3^- + Ca_2^+ \rightarrow CaCO_3 + H^+$

Skeleton

Acidosis across the calicoderm reduces the ability of coral host cells to calcify (50). We propose that under low pH conditions enhanced expression of carbonic anhydrase transports and reverses HCO_3^- hydration (a.k.a. carbonate dehydratase) to increase CO_2 availability for photosynthesis. This increase in CO_2 could compensate for the expected loss in CO_2 from host respiration that is suppressed at high temperatures (51), which may be insufficient to support photosynthesis, even at low algal endosymbiont density.

Although apoptotic cell death and autophagy are widely favored as the cellular mechanisms for coral bleaching, no effector proteins of either pathway, other than the multipurpose autophagy chaperone HSP70, could be detected in datasets from our experimental stress treatments. Conversely, it has been shown elsewhere that the intracellular persistence of the Zx-containing symbiosome relies on either the exclusion or retention of small Rab-GTPase (ARF/SAR gene family) proteins, which are regulators of vesicular trafficking essential to cellular transport and docking with specific target membranes (52). Significantly, symbiosomes of the sea anemone *Aiptasia pulchella* enveloping healthy *Symbiodinium* were found to contain the stabilizing vesicle-associated membrane protein ApRab5 and lacked detectable levels of downstream effector ApRab7 and ApRab11 protein regulators of lysosome biogenesis (53), whereas in symbiosomes having thermally impaired zooxanthellae, it was the ApRab5 protein that was missing and the downstream ApRab7 and ApRab11 proteins were present (54). Collectively, these data show that ApRab5 retention is a feature of host-symbiont communication for healthy symbionts to persist within the symbiosome of host cells and that ApRab5 is an antagonist of phagosomal maturation by the exclusion of downstream ApRab7 and ApRab11 proteins that direct the progression of phagocytosis (55). Therefore, ApRab arrest of symbiosome maturation is critical for preventing downstream, early-stage liposomal remodeling of the host-derived phagosomal membrane so that Zx-bearing symbiosomes are able to evade recognition by the innate immune system of the host (56) and thereby sustain

endosymbiosis. Thus, cellular communication and the cross-talk between Rab proteins and their effectors provide the coordination of endocytic pathways necessary to control organelle homeostasis (57) that in zooxanthellate corals has long been recognized as essential for host regulation of endosymbiont populations, which is central to the stability of the symbiosis.

We have previously reported proteomic evidence for exocytosis as a functional mechanism for the loss of endosymbionts from cnidarian host tissues in coral bleaching (16). For exocytosis to occur, there must be fusion of the tethered vesicle SNARE (vSNARE) protein with a membrane target SNARE (tSNARE) protein. This happens when Ca^{2+}-bound synaptogamin docks vSNARE and tSNARE proteins to release complexin from the SNARE complex, allowing vesicle fusion and exocytosis to proceed. Premature assembly of vSNARE and tSNARE in the absence of synaptogamin is prevented by calmodulin, which binds free calcium in the cell to clamp SNARE fusion. Rapid exocytosis is triggered by synaptogamin having a greater affinity for calcium than does calmodulin. A drop in intracellular pH of the calicoblastic epithelium and sub-calicoblastic medium has been shown in *S. pistillata* to reduce calcification upon seawater acidification (58). However, this treatment evoked only a gradual decrease in intracellular pH suggesting that *S. pistillata* can regulate its internal pH. It has yet to be determined if a transient shift in pH, perhaps by enhanced carbonic anhydrase activity at the tissue-skeleton interface, would be sufficient to cause $CaCO_3$ desorption, releasing free Ca_2^+ that on crossing into the gastrodermis might initiate exocytosis. While calcium uptake is largely regulated by photosynthesis (59), processes controlled by Ca_2^+ ion signaling in coral physiology is under reported and worthy of attention.

Our coral host protein data set shows high expression of tSNARE and synaptogamin but low expression of vSNARE and calmodulin. This is consistent with the host having the capacity to execute rapid symbiont exocytosis. As expected, there was no evidence of tSNARE or synaptogamin proteins expressed by algal endosymbionts nor, surprisingly, were vSNARE proteins found. We have suggested previously that endosymbiont-directed exocytosis could be a mechanism for "symbiont shuffling" of *Symbiodinium* clades (16). Not detecting vSNARE proteins might suggest that endosymbionts can only manipulate membrane fusion through expression of their own vSNARE proteins early in the bleaching process. We therefore posit that vSNARE protein expression triggers the onset of bleaching but is not expressed during late-stage bleaching by residual stress-resistant *Symbiodinium* that remain *in hospite*, and calmodulin is released to bind free calcium required by host-encoded synaptogamin to unclamp the SNARE complex assembly necessary for membrane fusion and, thus, terminate complete symbiont exocytosis. Proteomic experiments are now warranted whereby the process and timing of exocytosis can be more fully explored.

REFERENCES

1. Szmant, A. M., and Gassman, N. J. (1990) The effects of prolong "bleaching" on the tissue biomass and reproduction of the reef coral *Montastrea annulatis*. *Coral Reefs* **8,** 217–224
2. Ateweberhan, M., Feary, D. A., Keshavmurthy, S., Chen, A., Schleyer, M. H., and Sheppard, C. R. (2013) Climate change impacts on coral reefs: synergies with local effects, possibilities for acclimation, and management implications. *Mar. Pollut. Bull.* **74,** 526–539
3. Muscatine, L., and Pool, R. R. (1979) Regulation of numbers of intracellular algae. *Proc. R. Soc. B* **204,** 131–139
4. Gates, R. D., Baghdasarian, G., and Muscatine, L. (1992) Temperature stress causes host cell detachment in symbiotic cnidarians: implications for coral bleaching. *Biol. Bull.* **182,** 324–332
5. Dunn, S. R., Schnitzler, C. E., and Wies, V. M. (2007) Apoptosis and autophagy as mechanisms of dinoflagellate symbiont release during cnidarian bleaching: Every which way you lose. *Proc. Biol. Soc.* **274,** 3079–3085
6. Ainsworth, T. D., and Hoegh-Guldberg, O. (2008) Cellular processes of bleaching in the Mediterranean coral *Oculina patagonica. Coral Reefs* **27,** 593–597
7. Sammarco, P. W., and Strychar, K. B. (2009) Effects of climate change/global warming on coral reefs: Adaptation/exaptation in corals, evolution in zooxanthellae, and biogeographic shifts. *Env. Bioindicators* **4,** 9–45
8. Brown, B. E., Le Tissier, M. D. A., and Bythell, J. C. (1995) Mechanisms of bleaching deduced from histological studies of reef samples during a natural bleaching event. *Mar. Biol.* **122,** 655–663
9. Bhagooli, R., and Hidaka, M. (2004) Photoinhibition, bleaching susceptibility and mortality in two scleractinian corals, *Platygyra ryukyuensis* and *Stylophora pistillata*, in response to thermal and light stresses. *Comp. Biochem. Physiol. A Mol. Integr. Physiol.* **137,** 547–555
10. Fang, L.-S., Huang, S-P., and Lin, K-L. (1997) High temperature induces the synthesis of heat-shock proteins and the elevation of intracellular calcium in the coral *Acropora grandis. Coral Reefs* **16,** 127–131
11. Ralph, P. J., Larkum, A. W. D., and Kühl, M. (2005) Temporal patterns in effective quantum yield of individual zooxanthellae expelled during bleaching. *J. Exp. Marine Biol. Ecol.* **316,** 17–28
12. Burgoyne, R. D., and Morgan, A. (1998) Calcium sensors in regulated exocytosis. *Cell Calcium* **24,** 367–376
13. DeSalvo, M. K., Voolstra, C. R., Sunagawa, S., Schwarz, J. A., Stillman, J. H., Coffroth, M. A., Szmant, A. M., and Medina, M. (2008) Differential gene expression during thermal stress and bleaching in the Caribbean coral *Montastraea faveolata. Mol. Ecol.* **17,** 3952–3971
14. Starcevic, A., Dunlap, W. C., Cullum, J., Shick, J. M., Hranueli, D., and Long, P. F. (2010) Gene expression in the scleractinian *Acropora mi-*

crophthalma exposed to high solar irradiance reveals elements of photoprotection and coral bleaching. *PLoS One* **5,** e13975

15. Burgoyne, R. D., and Clague, M. J. (2003) Calcium and calmodulin in membrane fusion. *Biochim. Biophys. Acta* **1641,** 137–143

16. Weston, A. J., Dunlap, W. C., Shick, J. M., Klueter, A., Iglic, K., Vukelic, A., Starcevic, A., Ward, M., Wells, M. L., Trick, C. G., and Long, P. F. (2012) A profile of an endosymbiont-enriched fraction of the coral *Stylophora pistillata* reveals proteins relevant to microbial-host interactions. *Mol. Cell Proteomics* 11, M111.015487

17. Dunlap, W. C., Starcevic, A., Baranasic, D., Diminic, J., Zucko, J., Gacesa, R., van Oppen, M. J., Hranueli, D., Cullum, J., and Long, P. F. (2013) KEGG orthology-based annotation of the predicted proteome of *Acropora digitifera*: ZoophyteBase—An open access and searchable database. *BMC Genomics* **14,** 509

18. Lesser, M. P. (2006) Oxidative stress in marine environments: Biochemistry and physiological ecology. *Annu. Rev. Physiol.* **68,** 253–278

19. Sawyer, S. J., and Muscatine, L. (2001) Cellular mechanisms underlying temperature-induced bleaching in the tropical sea anemone *Aiptasia pulchella*. *J. Exp. Biol.* **204,** 3443–3456

20. Huang, S.-P., Lin, K.-L., and Fang, L.-S. (1998) The involvement of calcium in heat-induced coral bleaching. *Zool. Stud.* **37,** 89–94

21. Veron, J. E. N., and Wallace, C. C. (1984) Scleractinia of eastern Australia part 5, *Acroporidae*. *Aus. Inst. Mar. Sci. Monogr. Ser.* 6, 485 pp.

22. Ulstrup, K. E., and Van Oppen, M. J. (2003) Geographic and habitat partitioning of genetically distinct zooxanthellae (*Symbiodinium*) in *Acropora* corals on the Great Barrier Reef. *Mol. Ecol.* **12,** 3477–3484

23. Jones, A. M., Berkelmans, R., van Oppen, M. J., Mieog, J. C., and Sinclair, W. (2008) A community change in the algal endosymbionts of a scleractinian coral following a natural bleaching event: Field evidence of acclimatization. *Proc. Biol. Sci.* **275,** 1359–1365

24. Laemmli, U. K. (1970) Cleavage of structural proteins during the assembly of the head of bacteriophage T4. *Nature* **227,** 680–685

25. Schevchenko, V. A., Akayeva, E. A., Yeliseyeva, I. M., Yelisova, T. V., Yofa, E. L., Nilova, I. N., Syomov, A. B., and Burkart, W. (1996) Human cytogenetic consequences of the Chernobyl accident. *Mutat. Res.* **361,** 29–34

26. Shoguchi, E., Shinzato, C., Kawashima, T., Gyoja, F., Mungpakdee, S., Koyanagi, R., Takeuchi, T., Hisata, K., Tanaka, M., Fujiwara, M., Hamada, M., Seidi, A., Fujie, M., Usami, T., Goto, H., Yamasaki, S., Arakaki, N., Suzuki, Y., Sugano, S., Toyoda, A., Kuroki, Y., Fujiyama, A., Medina, M., Coffroth, M. A., Bhattacharya, D., and Satoh, N. (2013) Draft assembly of the *Symbiodinium minutum* nuclear genome reveals dinoflagellate gene structure. *Curr. Biol.* **23,** 1399–1408

27. Beltran, V. H., Dunlap, W. C., and Long, P. F. (2012) Comparison of the photosynthetic bleaching response of four coral species common to the central GBR. In *Proceedings of the 12th International Coral Reef Symposium.* From: 12th International Coral Reef Symposium, 9–13 July 2012, Cairns, QLD, Australia.

28. Weis, V. V., and Levine, R. (1996) Differential protein profiles reflect the different lifestyles of symbiotic and aposymbiotic *Anthopleura elegantissima*, a sea anemone from temperate waters. *J. Exp. Biol.* **199,** 883–892

29. Barneah, O., Benayahu, Y., and Weis, V. M. (2006) Comparative proteomics of symbiotic and aposymbiotic juvenile soft corals. *Mar. Biotechnol.* **8,** 11–16

30. de Boer, M. L., Krupp, D. A., and Weis, V. M. (2007) Proteomics and transcriptional analyses of coral larvae newly engaged in symbiosis with dinoflagellates. *Comp. Biochem. Physiol. D Genom. Proteomics* **2,** 63–73

31. Peng, S.-E., Wang, Y.-B., Wang, L.-H., Chen, W.-N., Lu, C.-Y., Fang, L.-S., and Chen, C.-S. (2010) Proteomic analysis of symbiosome membranes in Cnidaria-dinoflagellate endosymbiosis. *Proteomics* **10,** 1002–1016

32. Schreiber, U. (2004) Pulse amplitude modulation (PAM) fluorometry and saturation pulse method: an overview. Papageorgiou, G. C. (ed). In *Chlorophyll a fluorescence: A signature of photosynthesis.* Dordrecht: Kluwer Academic. Chapter 11, pp. 279–319

33. Kühl, M., Cohen, Y., Dalsgaard, T., Jørgensen, B. B., and Revsbech, N. P. (1995) Microenvironment and photosynthesis of zooxanthellae in scleractinian corals studied with microsensors for O₂, pH and light. *Mar. Ecol. Prog. Ser.* **117,** 159–172

34. Dykens, J. A., Shick, J. M., Benoit, C., Buettner, G. R., and Winston, G. W. (1992) Oxygen radical production in the sea anemone *Anthopleura el-*

egantissima and its endosymbiotic algae. *J. Exp. Biol.* **168,** 219–241

35. Baird, A. H., Bhagooli, R., Ralph, P. J., and Takahashi, S. (2009) Coral bleaching: the role of the host. *Trends Ecol. Evol.* **24,** 16–20

36. Shick, J. M., and Dykens, J. A. (1985) Oxygen detoxification in algal-invertebrate symbioses from the Great Barrier Reef. *Oecologia* **66,** 33–41

37. Shick, J. M., Lesser, M. P., Dunlap, W. C., Stochaj, W. R., Chalker, B. E., and Won, J. W. (1995) Depth-dependent responses to solar ultraviolet-radiation and oxidative stress in the zooxanthellate coral *Acropora microphthalma*. *Mar. Biol.* **122,** 41–51

38. Hayward, D. C., Hetherington, S., Behm, C. A., Grasso, L. C., Forêt, S., Miller, D. J., and Ball, E. E. (2011) Differential gene expression at coral settlement and metamorphosis—A subtractive hybridization study. *PLoS One* **6,** e26411

39. DeLange, R. J., and Glazer, A. N. (1990) Bile acids: antioxidants or enhancers of peroxidation depending on lipid concentration. *Arch. Biochem. Biophys.* **276,** 19–25

40. Nichino, T., Okamoto, K., Eger, B. T., Pai, E. F., and Nishino, T. (2008) Mammalian xanthine oxidoreductase—mechanism of transition from xanthine dehydrogenase to xanthine oxidase. *FEBS J.* **275,** 3278–3289

41. Laurent, J., Tambutté, S., Tambutté, É., Allemand, D., and Venn, A. (2013) The influence of photosynthesis on host intracellular pH in scleractinian corals. *J. Exp. Biol.* **216,** 1398–1404

42. Gibbin, E. M., Putnam, H. M., Davy, S. K., and Gates, R. D. (2014) Intracellular pH and its response to CO₂-driven seawater acidification in symbiotic *versus* non-symbiotic coral cells. *J. Exp. Biol.* **217,** 1963–1969

43. Furla, P., Galgani, I., Durand, I., and Allemand, D. (2000) Sources and mechanisms of inorganic transport for coral calcification and photosynthesis. *J. Exp. Mar. Biol. Ecol.* **203,** 3445–3457

44. Al-Horani, F. A., Al-Moghrabi, S. M., and de Beer, D. (2003) Microsensor study of photosynthesis and calcification in the scleractinian coral, *Galaxea fascicularis*: Active internal carbon cycle. *J. Exp. Mar. Biol. Ecol.* **288,** 1–15

45. Moya, A., Tambutté, S., Bertucci, A., Tambutté, E., Lotto, S., Vullo, D., Supuran, C. T., Allemand, D., and Zoccola, D. (2008) Carbonic anhydrase in the scleractinian coral *Stylophora pistillata*: Characterization, localization, and role in biomineralization. *J. Biol. Chem.* **283,** 25475–25484

46. Tambutté, E., Tambutté, S., Segonds, N., Zoccola, D., Venn, A., Erez, J., and Allemand, D. (2012) Calcein labelling and electrophysiology: insights on coral tissue permeability and calcification. *Proc. Biol. Sci.* **279,** 19–27

47. Weis, V. M., and Reynolds, W. S. (1999) Carbonic anhydrase expression and synthesis in the sea anemone *Anthopleura elegantissima* are enhanced by the presence of dinoflagellate symbionts. *Physiol. Biochem. Zool.* **72,** 307–316

48. Bertucci, A., Moya, A., Tambutté, S., Allemand, D., Supuran, C. T., and Zoccola, D. (2013) Carbonic anhydrases in anthozoan corals—A review. *Bioorg. Med. Chem.* **21,** 1437–1450

49. Jokiel, P. L. (2011) The reef coral two compartment proton flux model: A new approach relating tissue-level physiological processes to gross corallum morphology. *J. Exp. Mar. Biol. Ecol.* **409,** 1–12

50. Venn, A. A., Tambutté, E., Lotto, S., Zoccola, D., Allemand, D., and Tambutté, S. (2009) Intracellular pH in symbiotic cnidarians. *Proc. Natl. Acad. Sci. U.S.A.* **106,** 16574–16579

51. Agostini, S., Fujimura, H., Higuchi, T., Yuyama, I., Casareto, B. E., Suzuki, Y., and Nakano, Y. (2013) The effects of thermal and high-CO₂ stresses on the metabolism and surrounding microenvironment of the coral *Galaxea fascicularis*. *Coral Reef Biol.* **336,** 384–391

52. Deneka, M., Neeft, M., and van der Sluijs, P. (2003) Regulation of membrane transport by Rab GTPases. *Crit. Rev. Biochem. Mol. Biol.* **38,** 121–142

53. Chen, M.-C., Cheng, Y.-M., Sung, P.-J., Kuo, C.-E., and Fang, L.-S. (2003) Molecular identification of Rab7 (ApRab7) in *Aiptasia pulchella* and its exclusion from phagosomes harboring zooxanthellae. *Biochem. Biophys. Res. Commun.* **308,** 586–595

54. Chen, M.-C., Cheng, Y.-M., Hong, M.-C., and Fang, L.-S. (2004) Molecular cloning of Rab5 (ApRab5) in *Aiptasia pulchella* and its retention in phagosomes harboring live zooxanthellae. *Biochem. Biophys. Res. Commun.* **324,** 1024–1033

55. Chen, M.-C., Hong, M.-C., Huang, Y.-S., Liu, M.-C., Cheng, Y.-M., and Fang, L.-S. (2005) ApRab11, a cnidarian homologue of the recycling regulatory protein Rab11, is involved in the establishment and mainte-

nance of the *Aiptasia-Symbiodinium* endosymbiosis. *Biochem. Biophys. Res. Commun.* **338,** 1607–1616

56. Brumell, J. H., and Scidmore, M. A. (2007) Manipulation of Rab GTPase function by intracellular bacterial pathogens. *Microbiol. Mol. Biol. Rev.* **71,** 636–652

57. Zerial, M., and McBride, H. (2001) Rab proteins as membrane organizers. *Nat. Rev. Mol. Cell Biol.* **2,** 107–117

58. Venn, A. A., Tambutté, E., Holcomb, M., Laurent, J., Allemand, D., and Tambutté, S. (2013) Impact of seawater acidification on pH at the tissue-skeleton interface and calcification in reef corals. *Proc. Natl. Acad. Sci. U.S.A.* **110,** 1634–1639

59. de Beer, D., Kühl, M., Stambler, N., and Vaki, L. (2000) A microsensor study of light enhanced Ca^{2+} uptake and photosynthesis in the reef-building hermatypic coral *Favia* sp. *Mar. Ecol. Prog. Ser.* **194,** 75–85